Bull Volcanol (2005) 67:170–185
DOI 10.1007/s00445-004-0371-9

RESEARCH ARTICLE

Rachel Teasdale · Dennis Geist · Mark Kurz · Karen Harpp

1998 Eruption at Volcán Cerro Azul, Galápagos Islands: I. Syn-Eruptive Petrogenesis

Received: 21 October 2002 / Accepted: 19 April 2004 / Published online: 25 September 2004

Abstract The 1998 eruption of Volcán Cerro Azul in the Galápagos Islands produced two intra-caldera vents and a flank vent that erupted more than 1.0×10^8 m^3 of lava. Lava compositions changed notably during the 5-week eruption, and contemporaneous eruptions in the caldera and on the flank produced different compositions. Lavas erupted from the flank vent range from 6.3 to 14.1% MgO, nearly the entire range of MgO contents previously reported from the volcano. On-site monitoring of eruptive activity is linked with petrogenetic processes such that geochemical variations are evaluated in a temporal context. Lavas from the 1998 eruption record two petrogenetic stages characterized by progressively more mafic lavas as the eruption proceeded. Crystal compositions, whole rock major and trace element compositions, and isotope ratios indicate that early lavas are the product of mixing between 1998 magma and remnant magma of the 1979 eruption. Intra-caldera lavas and later lavas have no 1979 signature, but were produced by the 1998 magma incorporating olivine and clinopyroxene xenocrysts. Thus, early magma petrogenesis is characterized by mixing with the 1979 magma, followed by the magma progressively entraining wehrlite cumulate mush.

Keywords Galápagos · Cerro Azul · Syneruptive Petrogenesis · Active Volcanism · Basalt

Editorial Responsibility: M.R. Carroll

R. Teasdale (✉)
Department of Geosciences,
California State University, Chico,
Chico, CA 95929, USA
e-mail: rteasdale@csuchico.edu
Tel.: +1-530-898-5547
Fax: +1-530-898-5234

D. Geist
Department of Geological Sciences,
University of Idaho,
Moscow, ID 83844-3022, USA

M. Kurz
Woods Hole Oceanographic Institution,
Woods Hole, MA 02543, USA

K. Harpp
Department of Geology,
Colgate University,
Hamilton, NY 13346, USA

Introduction

The 1998 eruption of Cerro Azul volcano offered an unprecedented opportunity to monitor the eruption of an active Galápagos volcano, because of early detection by the GOES satellite (Mouginis-Mark et al. 2000), the eruption's long duration, and relative accessibility of the vents and lava flows. Through fieldwork and remote sensing imagery, the eruptive events were documented from the first detection of the eruption through the final days of eruptive activity (Ellisor and Geist 1999; Mouginis-Mark et al. 2000). Samples were collected both during and after the eruption from well-documented locations whose time of emplacement is known.

The 1998 eruption produced lavas with a large compositional range, ranging from 6.3% MgO early in the eruption to 14.1% MgO at the end. The purpose of this paper is to describe the eruption, present mineral and whole rock compositions that reveal the petrogenetic history of the magma, and quantify the contributions of magmatic components. The results suggest that lavas erupted from the flank vent formed by progressive mixing between the parental magma and remnant magma from the 1979 eruption. The contribution of the 1979 magma progressively decreased and was followed by incorporation of exotic olivine and clinopyroxene crystals during the last two weeks of the eruption.

Although this is the first eruption in the Galapagos that has been studied well enough to document large intra-eruption compositional variations, of course it is not the first volcano to show such petrologic variations. Other eruptions, such as Pu'u O'o (e.g. Garcia et al. 1992, 1995), Mt. Pinatubo (e.g. Newhall and Punongbayan 1996), and Mt. St. Helens (e.g. Lipman and Mullineaux

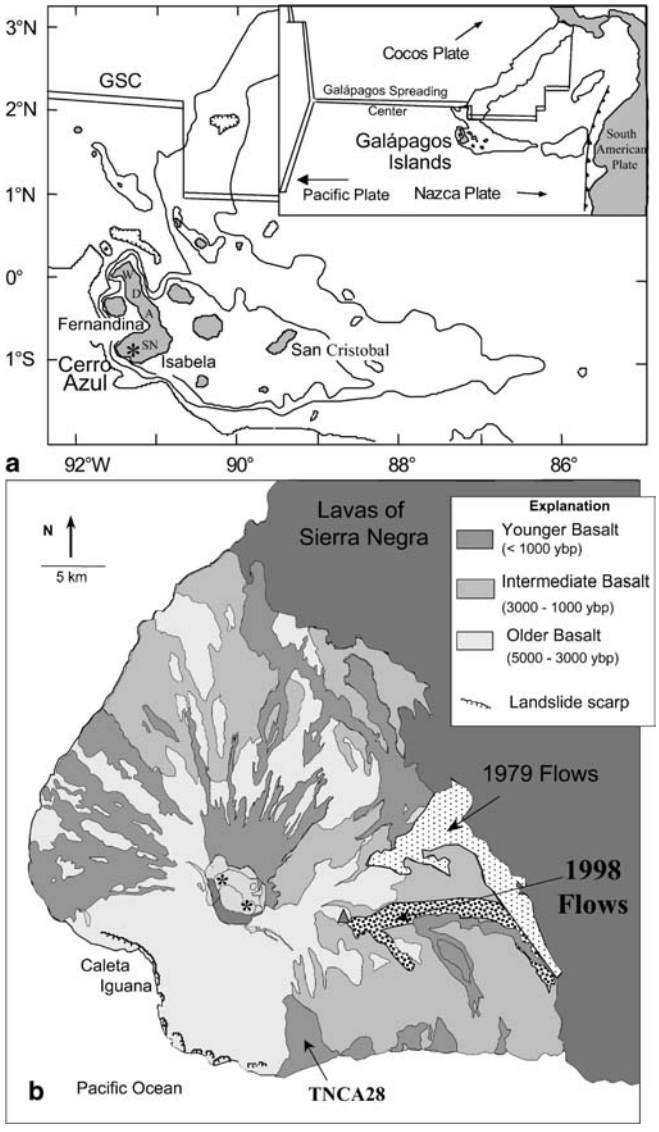

Fig. 1 a Galápagos Archipelago map with regional location map in inset. **b** Geologic Map of Volcán Cerro Azul. 1998 intracaldera vent locations are shown with *. Flank vent is shown with solid triangle. Locations of 1979 and 1998 flows are shown in fine and coarse stipple patterns, respectively. Pre-1998 geology from Naumann (1998)

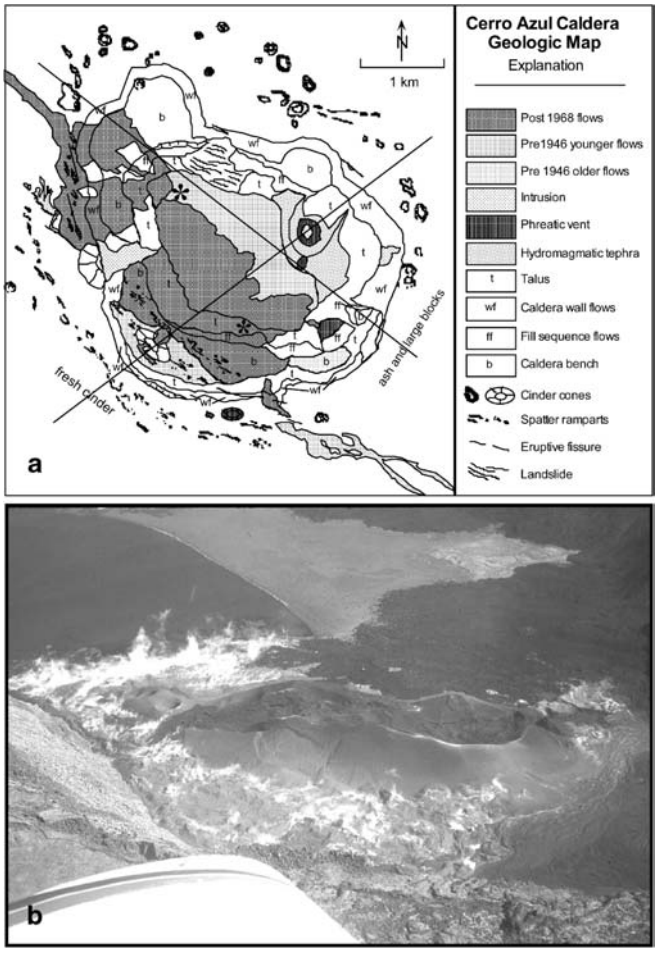

Fig. 2 a Geologic map of Cerro Azul caldera. The *s indicate western and southern vents of the 1998 eruption. Modified from Naumann (1998) **b** Intra-caldera vent, western end of caldera floor

1981), have played an important role in understanding the time scale of petrologic processes over the course of hours to years.

Brief history of the eruption

Cerro Azul is the southwestern-most volcano on Isla Isabela in the western Galápagos Islands (Fig. 1a), the region where most recent volcanic activity in the archipelago has occurred (Simkin and Siebert 2000). Recent detailed work at Cerro Azul volcano (Naumann 1998; Naumann and Geist 2000, Naumann et al. 2002) has provided an invaluable geologic and petrologic baseline on which to interpret the 1998 eruption. Those studies thoroughly characterized the eruptive history and petrology and geochemistry of pre-1998 lavas. Prior to 1998, the most recent activity at Cerro Azul occurred in 1979 when eruption from intra-caldera and flank vents resulted in the emplacement of lavas on the eastern flank of the volcano (Fig. 1b). On September 15, 1998, the GOES satellite detected eruptive activity within the caldera (Fig. 2a); eruptive activity on the southeastern flank of the volcano was then detected on September 16, 1998 (Mouginis-Mark et al. 2000).

Intra-caldera activity

At least two new vents were established inside the caldera of Cerro Azul in 1998, the largest being a NE-oriented fissure in the west end of the caldera floor (Fig. 2a,b). This vent built a chain of elongate cinder cones, with a combined length of approximately 750 m, from which lava erupted and traveled north-northeast, toward the northern caldera wall. Satellite monitoring indicates that

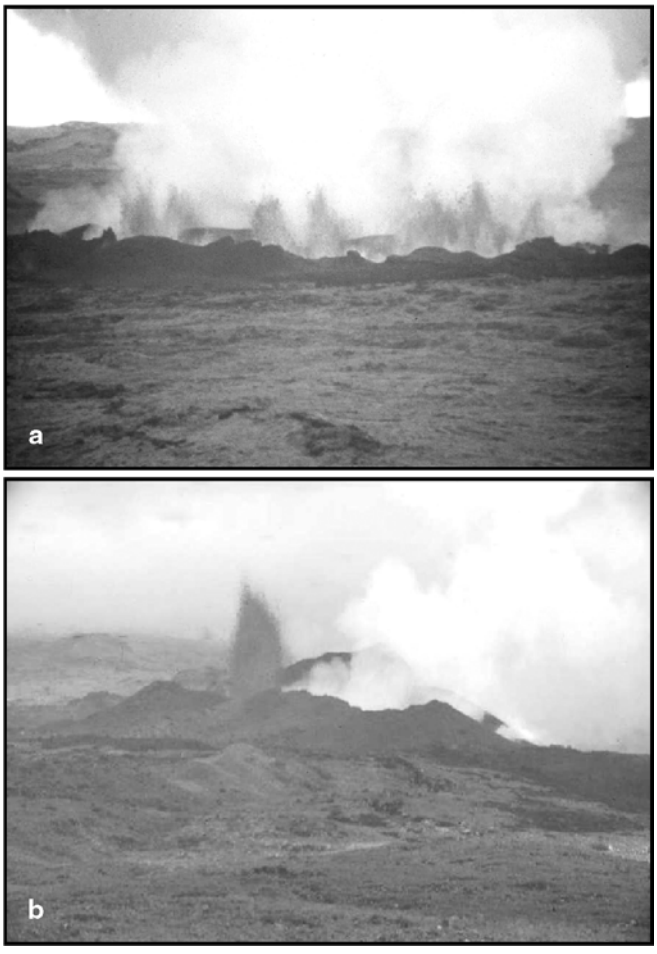

Fig. 3 a Flank vent, September 17, 1998; photo by Howard Snell. **b** Flank vent September 23, 1998; view faces NNE

the first intra-caldera activity was on September 15 (Mouginis-Mark et al. 2000).

The second intra-caldera vent is located on the southern bench (Fig. 2a), from which lava flowed north toward the southeastern caldera wall, then over the bench, cascading to the floor of the caldera. Spatter from the vent on the south bench covered the caldera wall above the vent, agglutinated, and flowed down the caldera wall to the floor. A third possible vent on the west end of the southern bench was not observed during fieldwork in 1998 nor by the GOES images, but was identified during fieldwork in 1999. By October 1, 1998, intra-caldera vents were no longer active except for gas emissions. Effusive activity from the intra-caldera vents can be constrained from GOES images and fieldwork to have lasted less than 17 days.

Flank activity

The flank activity started as a fissure eruption approximately 1 km in length (Fig. 3a; Ellisor 1998a, 1998b) that began erupting on September 16 (referred to as day 1 of the flank eruption). By day 7, fissure activity had built an elongate cone approximately 40 m in height (Fig. 3b). By day 17 of the eruption, the fissure focused to one main vent system with three small cones that fountained and issued lava. The final vent complex is approximately 80 m tall and 1 km in length.

Lava initially erupted from the southeastern (lower) end of the vent complex and simultaneously developed two main a'a flow lobes, each traveling southeast (Fig. 1b). The longest of the two flow lobes progressed east approximately 15 km from the vent, then banked against the 1979 flow, turned south and flowed an additional 5 km. The shorter of the two flows traveled southeast from the vent for approximately 7 km then turned south for an additional 3 km. The flows are up to 20 m thick.

Eruptive activity at the flank vent waned for 3–4 days during the fourth week of the eruption. The eruption then reactivated and became more vigorous for an additional two weeks, during which time short a'a and pahoehoe flow lobes erupted and flowed directly to the southwest. The second phase of eruptive activity corresponds to changes in both the compositions and surface morphology of the erupted lavas, as detailed below.

On the basis of mapping and remote sensing data, flows from the flank vent are estimated to have a volume of approximately 1.1×10^8 m^3 (P. Mouginis-Mark, personal communication). The long lavas that were emplaced early in the eruption are channelized a'a with well-developed flow levees. They contain rafted blocks up to 6 m in diameter, and large layered accretionary lava balls up to 4 m across. The later phase near-vent lavas are shorter flows dominated by a'a, but also include the only pahoehoe erupted from the flank vent. GOES satellite radiance data show heat anomalies that indicate the flank eruption continued until October 21, making the entire duration of eruptive activity 37 days (Mouginis-Mark et al. 2000).

Sampling and analyses

Thirty samples collected from the flank flows during and after the eruption were examined petrographically and analyzed for major and trace elements (Tables 1, 2, 3, 4). Samples erupted prior to day 18 of the eruption are referred to as "early erupted" lavas; those erupted from day 19 onward are referred to as "later erupted" flows. Two samples that are designated "transitional" erupted between the 18^{th} and 21^{st} days of the eruption.

Whole rock major and trace elements were determined at the Washington State University geoanalytical facility, using methods of Johnson et al. (1999). Additional trace element analyses by ICP-MS were completed at Colgate University, according to the methods described in Standish et al. (1998). Isotope analyses were completed at Woods Hole Oceanographic Institute using methods described by Kurz and Geist (1999).

Table 1 Lavas erupted from Cerro Azul in 1998: whole rock major element data

Sample	# Days after Eruption	Mg #	SiO_2	Al_2O_3	TiO_2	FeO	MnO	CaO	MgO	K_2O	Na_2O	P_2O_5	Total	CaO/Al_2O_3	Na_2O+K_2O
2	6	0.50	48.54	14.73	2.71	11.21	0.19	11.70	6.31	0.60	2.87	0.31	99.17	0.79	3.47
49	7	0.52	48.70	15.15	2.68	11.09	0.19	11.83	6.67	0.60	2.90	0.31	100.11	0.78	3.50
48B	7	0.52	48.85	15.08	2.68	10.88	0.19	11.93	6.65	0.61	2.92	0.30	100.09	0.79	3.53
1	8	0.53	48.13	15.10	2.57	11.19	0.18	11.87	7.12	0.58	2.86	0.29	99.89	0.79	3.44
5	11	0.57	48.29	15.32	2.33	10.57	0.18	12.18	8.02	0.52	2.62	0.27	100.30	0.80	3.14
6	11	0.57	48.36	15.49	2.34	10.57	0.17	12.27	7.88	0.52	2.64	0.27	100.51	0.79	3.16
7	12	0.57	47.78	15.58	2.22	10.35	0.17	12.43	7.78	0.50	2.61	0.25	99.67	0.80	3.11
8	12	0.57	48.36	15.68	2.33	10.43	0.17	12.39	7.60	0.53	2.71	0.27	100.46	0.79	3.24
52	12	0.57	48.41	15.56	2.40	9.91	0.17	12.37	7.24	0.54	2.65	0.27	99.52	0.79	3.19
45B	12	0.53	48.81	14.87	2.66	10.77	0.19	11.96	6.78	0.55	2.86	0.29	99.74	0.80	3.41
9	13	0.56	48.01	15.62	2.30	10.26	0.17	12.39	7.47	0.52	2.67	0.26	99.67	0.79	3.19
10	13	0.58	48.20	15.76	2.19	10.25	0.17	12.52	7.87	0.49	2.59	0.25	100.29	0.79	3.08
11	13	0.60	48.19	15.71	2.11	9.92	0.16	12.52	8.49	0.47	2.51	0.24	100.32	0.80	2.98
14	18	0.66	47.81	15.26	1.85	9.37	0.16	12.49	10.12	0.44	2.30	0.21	100.01	0.82	2.74
50	19	0.69	47.79	15.12	1.63	9.18	0.15	12.36	11.69	0.37	2.03	0.18	100.50	0.82	2.40
14C	19	0.56	48.17	15.55	2.35	10.46	0.17	12.34	7.42	0.53	2.73	0.27	99.99	0.79	3.26
14D	19	0.56	48.12	15.47	2.35	10.51	0.17	12.28	7.42	0.53	2.70	0.27	99.82	0.79	3.23
14E	19	0.59	47.65	15.55	2.12	9.97	0.17	12.42	8.21	0.48	2.53	0.24	99.33	0.80	3.01
44	21	0.62	48.87	15.01	2.30	10.29	0.18	11.87	9.33	0.53	2.60	0.26	101.24	0.79	3.13
16	25	0.70	47.65	14.97	1.62	9.39	0.15	12.25	12.11	0.36	2.05	0.18	100.72	0.82	2.41
42	25	0.70	48.41	15.29	1.69	8.93	0.15	12.71	11.43	0.39	2.23	0.18	101.42	0.83	2.62
43	25	0.56	49.25	15.56	2.54	10.35	0.18	12.13	7.31	0.55	2.70	0.29	100.85	0.78	3.25
41A	26	0.71	46.96	14.52	1.59	9.32	0.15	12.00	12.59	0.35	1.95	0.17	99.61	0.83	2.30
46	27	0.71	47.65	14.60	1.59	9.23	0.15	12.05	12.50	0.36	2.00	0.17	100.31	0.83	2.36
47	27	0.71	47.74	14.72	1.61	9.11	0.16	12.04	12.40	0.36	2.02	0.17	100.32	0.82	2.38
53	29	0.71	47.31	14.61	1.61	8.97	0.15	12.10	12.45	0.35	1.91	0.17	99.63	0.83	2.26
54	29	0.71	47.44	14.33	1.61	9.37	0.16	11.87	12.91	0.35	1.93	0.17	100.14	0.83	2.28
45a	post 19	0.70	47.12	14.93	1.62	8.91	0.15	12.26	11.61	0.36	1.98	0.18	99.11	0.82	2.34
Intracaldera Scoria	0–17	0.73	47.65	14.04	1.61	9.33	0.16	11.71	14.11	0.36	2.04	0.17	101.18	0.83	2.40
1979		0.49	48.37	14.99	3.02	11.47	0.19	11.20	6.28	0.69	3.41	0.36	100.00	0.75	4.11
TN-CA28		0.65	48.22	15.78	1.81	8.97	0.15	12.90	9.31	0.35	2.34	0.18	100.00	0.82	9.65

Table 2 Lavas erupted from Cerro Azul in 1998: trace element data (XRF)

Sample	Ni	Cr	Sc	V	Ba	Rb	Sr	Zr	Y	Nb	Ga	Cu	Zn	Pb	La xrf	Ce	Th
2																	
49	73	113	28	350	136	11	358	162	30	26	21	90	94	16	13	55	0
48B	81	136	34	343	151	11	350	161	30	25	20	93	94	1	19	46	1
1	102	175	43	341	108	11	354	158	29	24	21	99	99	0	3	36	0
5	132	245	33	305	91	10	344	140	26	21	20	92	88	7	6	55	1
6	126	264	32	320	90	9	348	142	26	22	22	87	89	3	23	37	0
7	126	293	33	312	91	9	350	134	24	20	20	79	84	0	18	37	2
8	113	258	29	321	99	11	352	141	26	22	20	92	88	0	3	31	1
52	104	231	30	324	126	9	351	141	26	21	21	92	88	2	15	31	4
45B	75	105	27	347	130	9	348	157	29	24	21	83	94	3	18	44	1
9	114	256	31	309	100	10	353	140	26	22	20	90	88	0	3	51	1
10	133	325	30	304	87	8	350	134	25	21	19	89	82	1	20	44	1
11	156	363	31	292	93	9	346	126	24	18	20	88	82	1	15	29	3
14	234	624	29	265	78	8	323	112	20	18	18	101	76	2	3	20	0
50	306	788	25	238	95	5	305	97	19	15	18	80	74	1	10	24	0
14C	119	253	34	312	96	10	351	143	26	20	18	95	93	0	0	30	1
14D	142	233	34	315	92	9	351	143	27	23	17	91	88	4	22	26	0
14E	156	366	33	295	83	11	348	128	23	20	19	95	83	0	6	39	1
44	196	480	33	316	124	8	337	138	25	20	20	85	86	4	11	41	2
16	322	783	26	229	80	7	302	96	19	14	16	82	74	0	9	13	3
42	286	920	28	246	94	7	313	101	20	16	16	79	73	2	19	43	2
43	119	340	30	335	121	12	348	152	27	22	17	96	100	0	10	42	2
41A	345	799	32	236	88	6	298	95	19	13	16	78	71	0	13	42	1
46	348	811	30	229	93	7	294	94	19	15	16	79	73	3	18	24	2
47	342	802	25	236	108	5	296	94	19	16	19	78	72	8	15	31	2
53	356	865	30	234	93	6	298	93	18	14	17	76	76	0	0	29	0
54	359	914	28	235	80	5	293	94	20	14	18	78	71	0	0	23	0
45a	309	802	33	235	94	6	305	97	20	15	13	80	70	1	15	46	2
Intracaldera Scoria	393	1049	26	237	85	6	286	94	19	13	18	73	73	3	27	29	0
1979	47	106	33	367	150	13	383	187	31	32		69	104				
TN-CA28	173	511	47	255	48	6	321	110	20	16		80	72	1	11	24	1

Table 3 Lavas erupted from Cerro Azul in 1998: trace element data (ICP)

Sample	Ba	La	Ce	Pr	Nd	Sm	Eu	Gd	Tb	Dy	Ho	Er	Tm	Yb	Lu	Hf	U	La/Sm
2																		
49																		
48B																		
1	140	17	38	5	22	5	2	5	0.9	5	1.0	2.7	0.4	2.3	0.3	3.6	0.4	3.3
5	133	16	36	5	21	5	2	5	0.8	5	0.9	2.5	0.4	2.1	0.3	3.3	0.4	3.3
6																		
7																		
8	134	16	36	5	21	5	2	5	0.8	5	0.9	2.5	0.4	2.1	0.3	3.3	0.4	3.3
52																		
45B	92	11	24	3	14	3	1	4	0.6	3	0.7	1.9	0.3	1.6	0.2	2.3	0.2	3.1
9																		
10	127	15	34	5	20	5	2	5	0.8	4	0.9	2.4	0.3	2.0	0.3	3.2	0.4	3.3
11	124	15	33	4	19	5	1	5	0.8	4	0.9	2.4	0.3	2.0	0.3	3.0	0.4	3.2
14	118	14	30	4	18	4	1	4	0.7	4	0.8	2.2	0.3	1.8	0.3	2.8	0.3	3.3
50	138	17	37	5	22	5	2	5	0.9	5	1.0	2.7	0.4	2.3	0.3	3.6	0.4	3.2
14C																		
14D																		
14E																		
44	154	19	43	6	25	6	2	6	1.0	6	1.1	3.0	0.4	2.5	0.4	4.0	0.5	3.2
16	94	11	24	3	14	3	1	4	0.6	3	0.7	1.9	0.3	1.6	0.2	2.3	0.3	3.1
42	94	11	24	3	14	4	1	4	0.6	3	0.7	1.9	0.3	1.6	0.2	2.3	0.3	3.1
43																		
41A																		
46																		
47																		
53																		
54	94	11	24	3	14	4	1	4	0.6	3	0.7	1.9	0.3	1.6	0.2	2.4	0.3	3.1
45a																		
Intracaldera Scoria	130	17	38	5	23	5	2	6	0.9	5	1.0	2.8	0.4	2.4	0.3	3.7	0.4	3.1
1979																		
TN-CA28	83	11	24	3	15	4	1	4	0.7	4	0.8	2.2	0.3	1.6	0.2	2.7	0.3	2.8

Table 4 Lavas erupted from Cerro Azul in 1998: Trace element ratios and isotope ratios

Sample	Sr/Zr	Sc/Y	Ba/Nb	Ba/Nb	Nb/Zr	Sm/Yb	Sc/Yb	Ba/Rb	K/Rb	Sc/Zr	$^{87}Sr/^{86}Sr$	2sigma 87/86	$^{3}He/^{4}He$	2sigma He
2														
49	2.21	0.93	5.29	5.29	0.16				453	0.17	0.703377	0.000014	12.84	0.16
48B	2.17	1.13	5.99	5.99	0.16				460	0.21				
1	2.24	1.48	4.60	4.60	0.15	2.3	18.6	12.8	438	0.27				
5	2.46	1.27	4.27	4.27	0.15	2.3	15.4	13.3	432	0.24				
6	2.45	1.23	4.17	4.17	0.15				480	0.23				
7	2.61	1.38	4.64	4.64	0.15				461	0.25				
8	2.50	1.12	4.58	4.58	0.15	2.3	13.6	12.2	400	0.21				
52	2.49	1.15	5.89	5.89	0.15				498	0.21				
45B	2.22	0.93	5.53	5.53	0.15	2.2	17.2	10.2	507	0.17				
9	2.52	1.19	4.59	4.59	0.16				432	0.22				
10	2.61	1.20	4.14	4.14	0.16	2.3	14.7	15.9	508	0.22				
11	2.75	1.29	5.08	5.08	0.15	2.3	15.8	13.8	434	0.25				
14	2.88	1.45	4.46	4.46	0.16	2.3	15.8	14.7	457	0.26	0.703330	0.000002	12.53	0.16
50	3.14	1.32	6.42	6.42	0.15	2.3	11.0	27.7	614	0.26				
14C	2.45	1.31	4.71	4.71	0.14				440	0.24	0.703365	0.000014	12.74	0.14
14D	2.45	1.26	4.00	4.00	0.16				489	0.24				
14E	2.72	1.43	4.19	4.19	0.15				362	0.26				
44	2.44	1.32	6.20	6.20	0.14	2.4	13.1	19.2	550	0.24				
16	3.15	1.37	5.80	5.80	0.14	2.2	16.7	13.5	427	0.27	0.703383	0.000013	13.30	0.18
42	3.10	1.40	6.03	6.03	0.15	2.2	17.9	13.5	463	0.28				
43	2.29		5.45	5.45	0.15				380	0.20				
41A	3.14	1.68	6.77	6.77	0.14				484	0.34				
46	3.13	1.58	6.20	6.20	0.16				427	0.32				
47	3.15	1.32	6.71	6.71	0.17				598	0.27				
53	3.20	1.67	6.89	6.89	0.15				484	0.32				
54	3.12	1.40	5.63	5.63	0.15	2.2	17.5	18.7	581	0.30				
45a	3.14	1.65	6.39	6.39	0.15				498	0.34				
Intracaldera Scoria	3.04	1.37	6.69	6.69	0.14	2.3	11.0	21.7	498	0.28	0.703369	0.000017		
1979	2.05	1.06	4.76	4.76	0.17				442	0.18	0.703404	0.000014		
TN-CA28	2.92	2.35	3.08	3.08	0.14	2.5	28.9	13.8	479	0.43				

Olivine, clinopyroxene, plagioclase, and Cr-spinel compositions were determined using the Washington State University Cameca Camebax electron microprobe and the University of Oregon CAMECA SX50 microprobe. A <5 μm diameter beam was used with a beam voltage of 15 kV and currents of about 10 nA.

Petrography/mineral chemistry

The 1998 lavas have a wide range of crystallinity, with between 2.4 and 38.5% total phenocrysts, defined here as crystals >1 mm in greatest dimension. Most samples are dominated by 2–20% phenocrysts of plagioclase with fewer phenocrysts of olivine (0.2 – 17%), clinopyroxene (0–10%) and microphenocrysts of Cr-spinel (up to 5.5%, defined here as 50–1000 μm in length).

Plagioclase phenocrysts are coarse-grained and subhedral to anhedral. Many form glomerocrysts with olivine and clinopyroxene and generally have ragged crystal faces. Some microphenocrysts (50–1000 μm) of plagioclase have swallowtail habits. In the early erupted lavas, many plagioclase cores are resorbed, some with glass inclusions in their interiors.

Plagioclase core and rim compositions range from An_{73} to An_{94}. The oldest and youngest groups of 1998 lavas have the smallest range of anorthite compositions (An_{85} to An_{91} and An_{90} to An_{94}, respectively); whereas samples of lavas erupted between days 19–25 tend to have plagioclase with broader compositional ranges (An_{73} to An_{92}). In general, plagioclase cores tend to be more anorthitic than the rims, but all lavas have examples of plagioclase crystals with both normal- and reverse-zoned phenocrysts. In nearly all cases, groundmass plagioclase has the lowest anorthite composition (An_{73} to An_{82}), similar to phenocryst rim compositions.

Olivine phenocrysts are most abundant and largest in the later erupted lavas, up to 1 cm in diameter in sample 16 (which erupted day 25). Many phenocrysts in later erupted lavas have kink bands and are highly fractured (Fig. 4a). Olivine phenocrysts in sample 14 (day 18) have abundant Cr-spinel inclusions in crystal cores that increase in abundance toward olivine rims, where they form clusters up to 130 μm thick (Fig. 4b). Nearly all of the olivine phenocrysts are single crystals; multi-crystal glomerocrysts and xenoliths are rare.

Olivine core and rim compositions range from Fo_{77} – Fo_{89}. Variations are greatest in the oldest and intermediate-aged lavas, whereas olivine compositions in younger lavas are limited to Fo_{83} – Fo_{86}. Most grains are normal zoned; approximately 15% of the measured olivines are reverse zoned. The relative age of samples (early erupted lavas vs. later erupted lavas) does not appear to correlate with zoning variations.

Clinopyroxene phenocrysts are relatively rare in early erupted lavas (<2% of the mode) but tend to be more abundant in later erupted lavas (up to 10%). Clinopyroxenes have Mg#s ranging from 74.4–87.2 and CaO from 19.9%–22.8%.

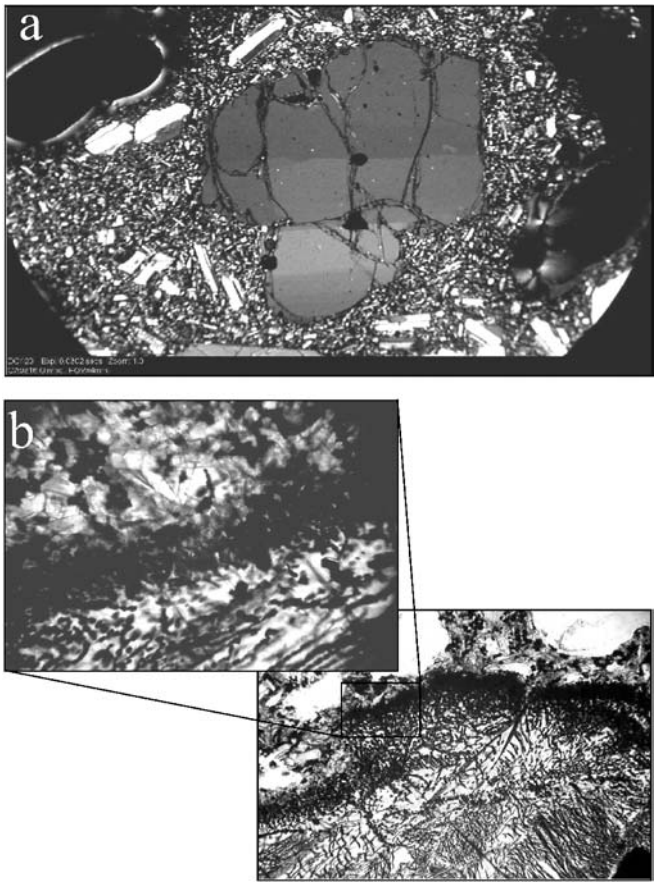

Fig. 4 a Kink banded olivine (undulose extinction zones) in sample 16. Field of view is 4 mm wide. **b** Sample 14 olivine with Cr-spinel inclusions. Upper view is 0.32 mm across, lower view is ~1 mm wide

Application of the Putirka et al. (1996) geobarometer to these pyroxene compositions is problematic, because the liquid compositions are unknown and most of the lavas have probably incorporated xenocrysts. If one assumes that the liquid from which the pyroxenes crystals formed had the composition of the proposed parental magma (sample TNCA28, see discussion below), then crystallization pressures of 7.6 ± 1.1 kb are obtained. We believe that these pressures are greater than the probable crystallization depth, because the pressure at the Moho in this area is <4 kb (Feighner and Richards 1994). Either our assumptions of liquid composition are incorrect (many were tried, with similar results), or the calibration is inappropriate for these compositions.

Cr-spinels are abundant in the groundmass of most samples and occur as microphenocrysts (50–1000 μm) and as inclusions in olivines in lavas with intermediate MgO content. They are rare in the later erupted samples. The greatest abundances of Cr-spinel occur in rocks with low abundances of clinopyroxene phenocrysts. Cr-spinels also occur in the groundmass of intermediate aged sample 14.

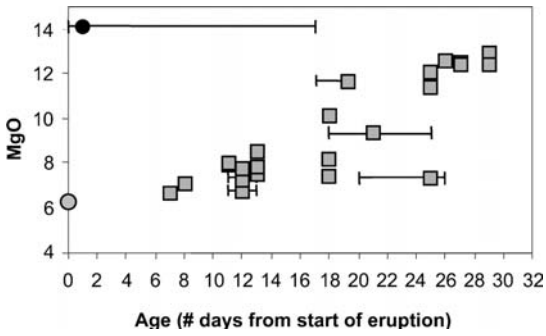

Fig. 5 1998 flank lava (gray squares) whole rock MgO *vs.* number of days after start of flank eruption (September 16, 1998) based on field observations. Elongate bars represent the range of time during which sample emplacement could have occurred for samples that were not collected the day they were emplaced. Gray circle shows the MgO composition of the 1979 magma present on day 0 of the eruption. The intracaldera composition is shown with a closed circle but the age is constrained only by the duration of the eruptions in the caldera having lasted 2 weeks (see text)

Major and trace element analyses

All lavas are tholeiitic basalts, and the lavas erupted from the flank vents are generally more mafic with time (Fig. 5 and Tables 1, 2, 3, 4). The precision of the MgO-time relationship for six samples that were collected in 1999 is limited, and the horizontal error bars shown on Fig. 5 show the range of possible eruptive days of these samples.

The compositional range of lavas from the 1998 eruption is extraordinary; whole rock compositions span nearly the entire range of known compositions from Cerro Azul, which is one of the most compositionally diverse of the western Galápagos shields (Naumann et al. 2002). The earliest-erupted 1998 lavas are compositionally similar to the volcano's most MgO-rich prehistoric lavas and are among the most primitive lavas within the entire western Galápagos Archipelago (White et al. 1993; Naumann et al. 2002).

The lavas form strongly curved arrays on plots of MgO versus Al_2O_3, FeO, CaO, and K_2O (Fig. 6), indicating that simple two-component mixing or assimilation is not responsible for the variations. Positive correlations occur between MgO and Al_2O_3, and MgO and CaO for the first-erupted lavas, whereas there are negative correlations in the younger lavas (Fig. 6). Increasing MgO correlates positively with Ni and Cr for all samples (Fig. 6g). All 1998 lavas have negative correlations between MgO and TiO_2, K_2O, Zr, Rb, Sr, Y, and Nb (Figs. 6 and 7). The $^{87}Sr/^{86}Sr$ and $^{3}He/^{4}He$ isotopic compositions of the 1998 lavas (Tables 1, 2, 3, 4) are nearly identical to the range reported for prehistoric Cerro Azul tholeiite lavas (Fig. 8; Kurz and Geist 1999; Naumann et al. 2002). Variation of $^{87}Sr/^{86}Sr$ is only slightly beyond analytical uncertainty but decreased with time through day 19 of the eruption, then increased. $^{3}He/^{4}He$ ratios in crushed olivine separates increased from 12.5 Ra to 13.5 Ra as the eruption progressed, which is within the range previously reported from the volcano but beyond analytical uncertainty.

Mineral-rock compositional relationships

Measured compositions of olivine crystals are compared to those predicted to be in equilibrium with whole rock compositions in Fig. 9 (using $K_d = 0.30 \pm 0.03$; Roeder and Emslie 1970). Olivine compositions are not related to whole rock compositions, because the average core composition is essentially the same in all lavas (Fig. 9). In general, olivines in the early erupted, low Mg# samples are too forsteritic for their whole rock compositions, and olivines in the later erupted, more mafic samples are too forsterite-poor for their whole rock Mg#. In contrast, sample 14 (erupted at an intermediate stage, with Mg# = 0.66) has core compositions that are in equilibrium with the whole rock Mg#. All olivines are likely to have crystallized at shallow levels, because they range from 0.24–0.39% CaO, well within the range of olivines considered to have crystallized at low pressure (e.g. Ulmer, 1989).

Petrogenetic constraints and modeling

Fractional crystallization and partial melting processes

Before discussing the processes most likely responsible for the secular variation of lava compositions in the 1998 eruption, we first show that neither simple fractionation of a single parental magma nor progressive partial melting of a homogeneous source can explain the observed trends.

Fractional crystallization

Although some of the compositional variations of the 1998 lavas suggest that the magmas are related by fractional crystallization of olivine, clinopyroxene, and plagioclase from a parental magma with >14% MgO, other evidence indicates that this is not the only process relating them. Sr/Zr ratios are consistent with fractionation of olivine and clinopyroxene to generate the later erupted lavas, and fractionation of all three phases to generate the earliest-erupted lavas (Fig. 10). MELTS fractionation calculations (Ghiorso and Sack 1995) that use the most mafic measured composition (14.1% MgO) as the parental magma, at mid-crustal depths (other studies indicate that Cerro Azul magmas undergo cooling and crystallization at ~ 2 kb; Geist et al. 1998; Naumann et al. 2002), successfully reproduce the compositions of the later erupted lavas but do not reproduce the compositions of the early lavas (Fig. 11). Fractionation would require a mechanism for erupting the most evolved magmas (6.3% MgO) prior to the more mafic magma (Fig. 5); clearly, the lavas are not related by progressive cooling and crystallization over the duration of the eruption. The possibility of a zoned magma body, with cooler, aphyric, evolved basalt overlying hotter, porphyritic more primitive basalt is unlikely because of the lack of correlation between whole rock and olivine compositions. In addition, mea-

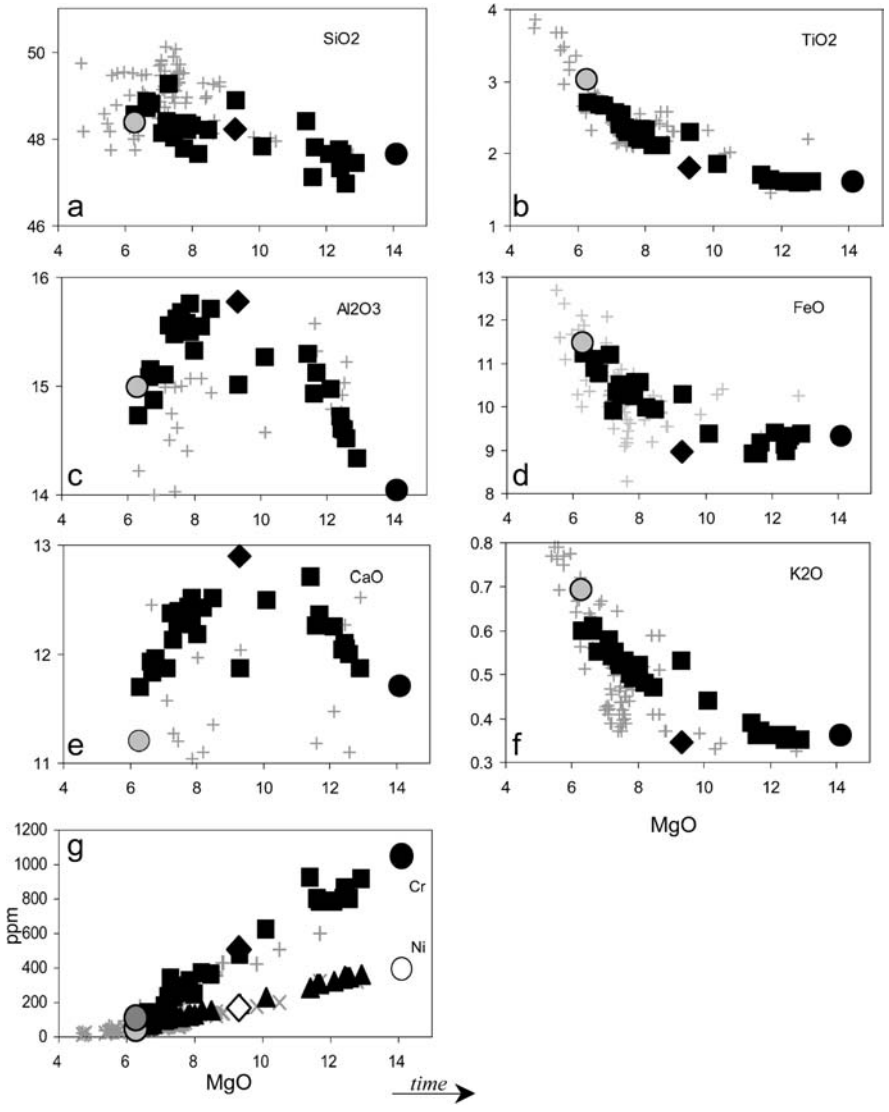

Fig. 6 a–f Major oxide variations *vs.* MgO. Closed squares are 1998 lavas, closed diamond is proposed parent composition (sample TNCA28) as described in text. Gray circle is 1979 composition; solid black circle is intracaldera scoria. Gray cross symbols are all previous samples from Cerro Azul (from Naumann 1998 and Naumann et al. 2002). **g** Compatible element variations *vs.* MgO for 1998 flank lavas. All symbols as noted above for Cr, except Ni 1998 lavas are shown with closed triangles, open diamond is TNCA28, open circle is intracaldera scoria, gray x symbols are all previous Ni analyses from Cerro Azul (from Naumann 1998 and Naumann et al. 2002)

surable variations in the isotopic ratios of Sr and He preclude simple crystal-liquid fractionation (Tables 1, 2, 3, 4).

Partial melting

Variations in major and trace element compositions through the course of single eruptions have also been attributed to progressive partial melting (e.g. Hoffmann et al. 1984; Garcia et al. 1996). Such a process would result in nearly constant concentrations of compatible trace elements, decreasing concentrations of incompatible trace elements, and decreasing La/Sm and La/Yb ratios with time (Reiners 2002). Incompatible element ratios indicative of progressive partial melting (e.g. La/Sm, La/Yb) do not vary systematically through the eruption (Fig. 7b). Thus, the compositional variations of the 1998 eruption cannot be explained by progressive extraction of partial melt from the mantle.

Compositional constraints on the parental magma

The 1998 eruption at Cerro Azul is the first basaltic eruption in the Galápagos Islands documented to have intra-eruption compositional variations (Volcán Alcedo erupted a zoned rhyolite-dacite; Geist et al. 1995a, 1995b).

The limited range of olivine compositions in the 1998 lavas is consistent with crystallization of most of the olivine from a relatively homogeneous parental magma. The average core composition of all measured olivines ($Fo_{85.5}$) corresponds to a parental liquid with an Mg# of 0.64, or approximately 10% MgO. The inflection of major element compositional trends occurs at approximately 10% MgO and 16% Al_2O_3, and is also the boundary between the early and later erupted lavas (Fig. 12). There is no such composition among the 1998 lavas, but a sample from a young flow on the south flank of Cerro Azul has the major element composition close to that of the inflection on a plot of MgO versus Al_2O_3 (sample TNCA28, Table 5). This flow is slightly vegetated, hence at least a

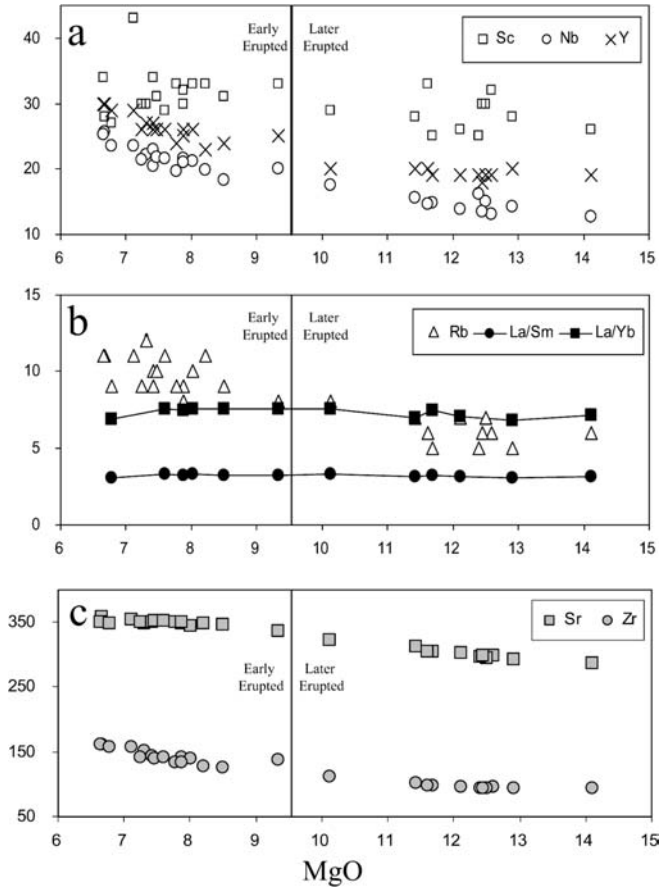

Fig. 7a–c MgO with incompatible elements **a** Sc, Nb, Y; **b** La/Sm and La/Yb; and **c** Incompatible elements Sr and Zr with MgO. Error bars for ratios are smaller than the size of symbols used, all analyses by XRF

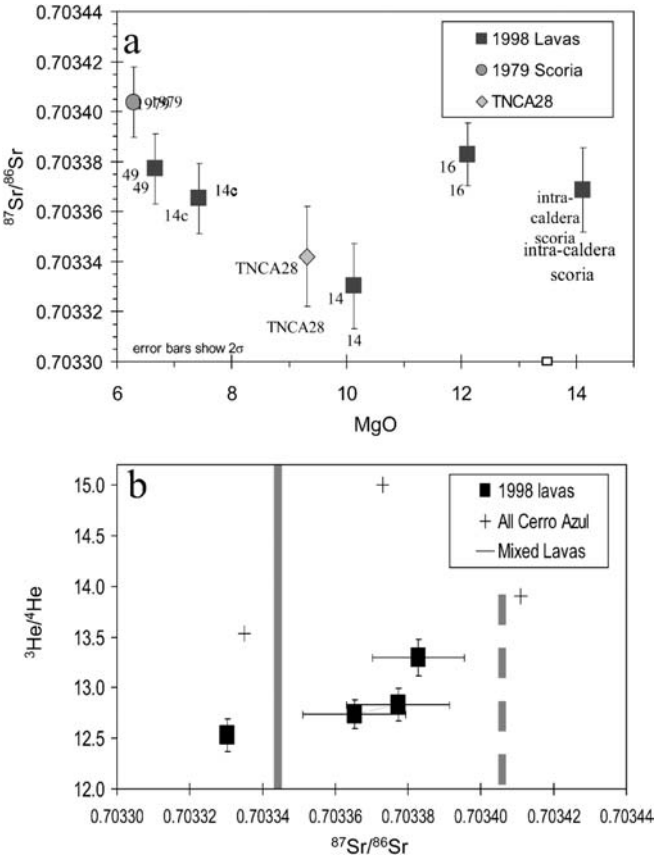

Fig. 8a,b Isotope ratios **a** $^{87}Sr/^{86}Sr$ vs. MgO for early (samples 49, 14c) intermediate (14) and later-erupted (16) lavas; **b** $^{3}He/^{4}He$ vs. $^{87}Sr/^{86}Sr$. Cross symbols represent isotope compositions of Cerro Azul lavas from Kurz and Geist (1999). Solid vertical bar represents $^{87}Sr/^{86}Sr$ value for sample TNCA28 (modeled as 1998 source magma) and dashed vertical bar represents $^{87}Sr/^{86}Sr$ value for 1979 magma. Error bars indicate 2σ

couple centuries old (Naumann 1998; Kurz and Geist, 1999), so it is unlikely that magma directly related to the lava flow from which TNCA28 was taken remained within the volcano by 1998, but sample TNCA28 simply represents a "typical" liquid composition that might repeatedly intrude into the shallow magmatic system.

Probable petrogenesis: magma mixing then crystal accumulation

We propose that the 1998 magma formed by two separate processes in which the early erupted lavas were generated when the parental magma with approximately 10% MgO (TNCA28) mixed with residual magma from the 1979 eruption. Once the last 1979 magma was flushed from the system, the magma began incorporating olivine and clinopyroxene crystals from a cumulate crystal mush zone, generating the later erupted lavas.

Early-erupted lavas, days 1–19

Major element variations, particularly Al_2O_3 and MgO, suggest that the early-erupted lavas result from mixing between the 1998 parental magma (composition similar to TNCA28) and remnant magma from the 1979 eruption (Fig. 12). Olivine zoning patterns provide important evidence for the mixing event. The range of olivine core compositions in the first-erupted magmas is much greater than in later erupted magmas, which suggests that olivines in the early erupted 1998 lavas crystallized in that magma but then mixed with the 1979 magma (Fig. 9). The equilibrium olivine composition for the 1979 liquid is Fo_{76} (Fig. 9). Samples 8 and 11 both have olivine grains that are close to this value (Fo_{78} and Fo_{77}) and erupted during the latter half of the early stage of the eruption (days 12 and 13). On this basis and age relations, we believe that the 1998 magma intersected the 1979 reservoir and progressively mixed with it (Fig. 13). Mass balance calculations suggest that the earliest lavas erupted in 1998 had very high proportions of 1979 magma (approximately 90%, Fig. 12). Subsequent lavas have

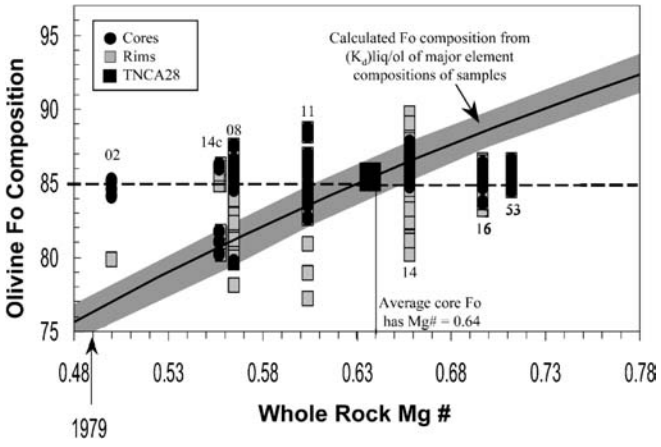

Fig. 9 Whole rock Mg # vs. forsterite composition (Fo = Mg/Fe+Mg in olivine). Gray field represents calculated values for olivine crystals that would be in equilibrium with liquids with Mg # of lava samples using Kd = 0.3 +/- 0.03 (Roeder and Emslie 1970). Gray squares represent rim compositions, filled circles are core compositions, and filled square is TNCA28 olivine composition from Naumann 1998. Mg # = whole rock Mg/Fe+Mg

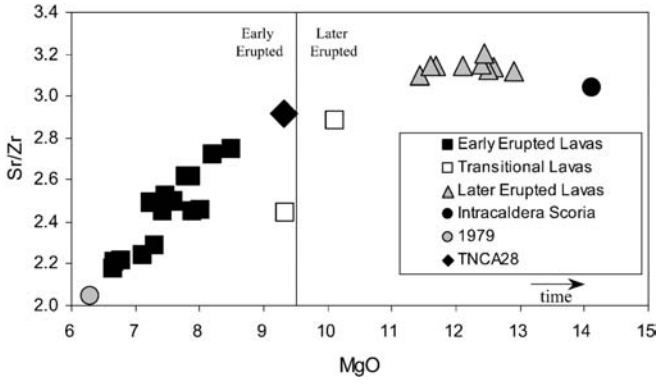

Fig. 10 Sr/Zr vs. MgO. Early erupted lavas are characterized by olivine, clinopyroxene, and plagioclase control; later erupted lava compositions characterized by olivine and clinopyroxene control. Gray circle represents 1979 composition, closed squares are 1998 early lavas, and gray triangles are later erupted lavas from 1998 eruption. Intermediate aged (transitional) lavas represented by open squares. Closed diamond is TNCA28, used to represent the composition of 1998 magma as described in text. Closed circle represents 1998 intra-caldera scoria composition

progressively decreasing proportions of 1979 magma, through at least day 19 of the eruption.

Mixing of the 1998 magma with the 1979 reservoir is also consistent with variations of Sr/Zr and CaO/Al_2O_3 with MgO (Figs. 10–12); calculated mixing curves closely match measured compositions of the earliest erupted 1998 lavas (lowest MgO on Fig. 12). Moreover, such an origin is consistent with the minor changes in Sr and He isotopic ratios. This would require that the parental 1998 magma and the remnant-1979 magmas had slightly different isotopic ratios. Because the proportion of the 1979 end member steadily decreases, mixing probably occurred during transport. Thus, physical mixing of the two batches

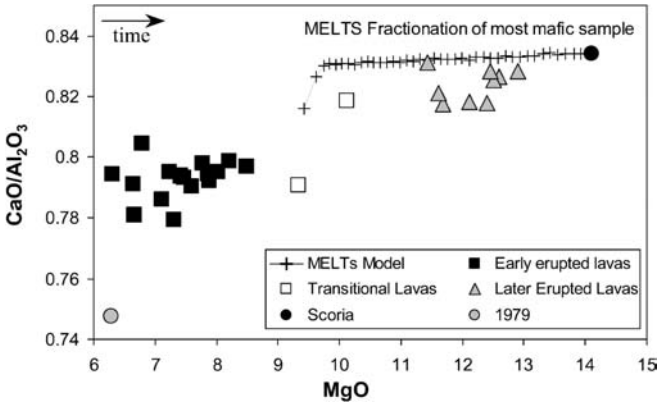

Fig. 11 CaO/Al_2O_3 vs. MgO with MELTS model for mafic (14.1% MgO) parent magma as described in text. Symbols for 1998 samples are the same as described in caption for Fig. 10. MELTS fractionation model shown by + symbols

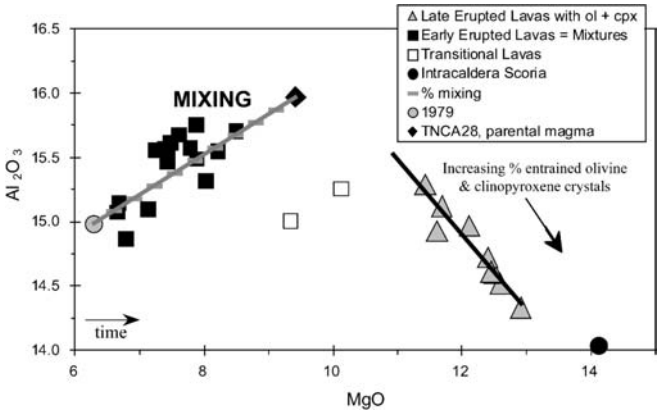

Fig. 12 Mixing and crystal incorporation models for petrogenesis of 1998 Cerro Azul lavas. Tick marks on mixing curve (gray line) represent 10% mixing increments between 1998 magma (TNCA28) and the 1979 magma. Increasing proportions of olivine and clinopyroxene are shown along the incorporation curve (black line). Symbols as described in Fig. 10

of magma may have occurred in the conduit as magma advanced towards the surface.

Later erupted lavas, day 19-end of eruption

Between the 19th and 25th day of the eruption, a change in eruptive style and volumetric flux accompanied a compositional shift in the lavas. By day 17, the intra-caldera vents were no longer active. By day 19 lava fountaining and flow activity at the flank vent were visibly diminished.

Intermediate-aged samples (14 and 44, Tables 1, 2, 3, 4) have major and trace element compositions intermediate to early and later erupted lavas. Lavas erupted after day 18 have higher MgO, Al_2O_3, and CaO than early erupted lavas. The timing also corresponds with a change in slope for most major and trace elements (e.g. Y, Rb, Sr, and Zr) (Tables 1, 2, 3, 4, Figs. 6 and 7). Analyzed lavas

Table 5 Mixing and crystal incorporation end member compositions

	Mixing		Crystal Incorporation		
	1979 Magma	1998 Magma	1998 Magma	Accumulated	Incorporated
	(DG-CA17)	(TN-CA28)	(TN-CA28)	Olivine	Clinopyroxene
Mg#	0.49	0.65	0.65	0.85	0.85
SiO_2	48.37	48.80	48.80	39.63	50.44
Al_2O_3	14.99	15.97	15.97	0.00	4.30
TiO_2	3.02	1.83	1.83	0.00	0.95
FeO*	11.47	9.08	9.08	13.94	5.01
MnO	0.19	0.15	0.15	0.20	0.08
CaO	11.20	13.05	13.05	0.36	21.93
MgO	6.28	9.42	9.42	44.82	15.62
K_2O	0.69	0.35	0.35	0.00	0.00
Na_2O	3.41	2.37	2.37	0.00	0.28
P_2O_5	0.36	0.18	0.18	0.00	0.00
Total	100.00	101.20	101.20	98.95	98.61

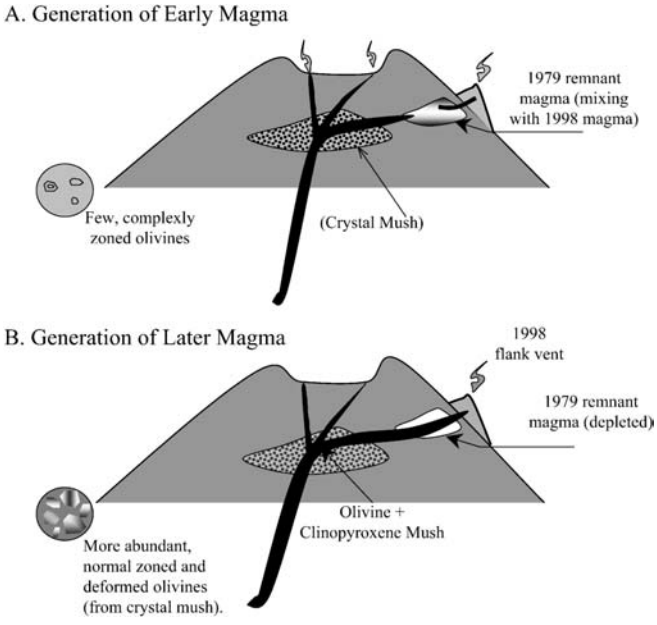

Fig. 13 Cartoon cross section of proposed petrogenetic model for the 1998 eruption at Cerro Azul

emplaced after day 18 do not indicate any compositional relationship to the 1979 magma. The compositions of these later-erupted lavas are instead indicative of progressive entrainment of olivine and clinopyroxene into the 1998 magma once the 1979 magma was flushed from the conduit. The modal proportions of olivine and clinopyroxene megacrysts increase with Mg# and order of erupted lavas. Sample 50 was the first of the later erupted lavas to be emplaced and has the lowest Mg# (0.69) and the lowest modal olivine (2.4%) and no clinopyroxene. Lavas erupted after sample 50 have increasing Mg#s and modal proportions of olivine (up to 17.1%) and clinopyroxene (up to 10.6%).

Compositional variations similar to those in the later erupted lavas at Cerro Azul have been attributed to progressive incorporation of olivine in Mauna Loa magmas (Garcia 1996; Rhodes 1996). In those rocks, olivine xenocrysts have kink bands but there is little compositional variation in the olivine crystals within single lavas (Garcia 1996). Entrainment of kink-banded olivine xenocrysts from cumulate zones has also been documented for xenocrysts described in Kilauea lavas (e.g. Helz 1987, Clague and Denlinger 1994, Clague et al. 1995). Similar xenocrystic textures are observed in olivines from the later erupted lavas of the 1998 Cerro Azul eruption (Fig. 4a).

Isotopic analyses of key samples from the 1998 eruption support the two-stage model presented here. The early erupted lavas from the 1998 eruption plot along mixing curves between the 1979 and the proposed parental 1998 magma (Fig. 12). The later erupted lava, sample 16, has more radiogenic $^{87}Sr/^{86}Sr$ and higher $^{3}He/^{4}He$ ratios, which suggest that the incorporated crystals did not crystallize from the parental 1998 magma. Sample 14 is intermediate aged and consistently plots beyond both the $^{87}Sr/^{86}Sr$ mixing curve and accumulation curves. This sample is anomalous and discussed below.

There are several possible sources for the crystals that became incorporated into magma that produced the later erupted lavas. Moderate CaO content in olivine phenocrysts suggests that they crystallized at fairly shallow levels (e.g. Ulmer 1989; Garcia et al. 1995). All measured olivine cores from later erupted lava samples have compositions within ~2% Fo (Fo_{84}-Fo_{86}), which constrains the liquid that crystallized them to range in Mg# between 0.60 and 0.66 (MgO = 8.2%–10.1%; Fig. 9). A cumulate crystal mush zone with appropriate olivine and clinopyroxene compositions could have formed prior to the 1998 eruption by crystallization from the proposed parental 1998 magma itself, or from an older magma. Crystallization from a parental magma with 10% MgO could have produced the crystals, which were then stored as a cumulate mush until day 25 of the eruption, when the original mafic liquid entrained the crystals and erupted as the later erupted lavas. We call on a "mush" because very few of the olivines occur in multigranular xenoliths; nearly all are as isolated single crystals.

Transitional lavas

The most difficult 1998 samples to explain are 44 and 14, both of which have intermediate MgO (9.33% and 10.12%, respectively), but Al_2O_3 compositions are lower than other 1998 lavas with equivalent MgO (Fig. 12). Both samples were collected from flows erupted between days 18 and 25, when we propose that the principal petrogenetic process shifted from mixing with 1979 magma to entrainment of crystals from a mush. Neither of the anomalous lavas can be modeled as the product of mixing (Fig. 12, open squares) between the 1979 and 1998 parental magmas. Moreover, crystal incorporation cannot reproduce either composition (Fig. 12). Sample 14 is unique in that it has olivine crystals that are riddled with spinel inclusions at their rims, which do not occur in olivine crystals of later erupted lavas (Fig. 4b). Thus, these two intermediate-aged magmas may have experienced both mixing and crystal assimilation processes or may result from incorporation of exotic magma and crystals not otherwise encountered by the 1998 parental magma.

Discussion

The two-stage process proposed here for the petrogenesis of the 1998 Cerro Azul lavas accounts for field observations, mineral compositions, modal abundances, and rock compositions. The transition from early mixing of the two magmas to eruption of less-modified 1998 magma is suggested by the decrease of the 1979 magma signature from day 1 through day 18. The triggering of crystal disaggregation and incorporation into the 1998 magma and the change in eruptive behavior is consistent with injection of a new pulse of the same parental magma after a slight lull in eruptive activity.

Physical constraints on mixing

Injection of the more mafic magma into the remnant 1979 magma reservoir provides a plausible explanation for the initiation of the 1998 flank eruption (e.g. Sparks et al. 1977). The orientation of a dike that fed the 1998 eruption can be estimated from the location of the intra-caldera and flank vents (Figs. 2a and 13). The flank vent is probably the result of radial dike emplacement (Chadwick and Howard 1991, Chadwick and Dietrich 1995). Simultaneous eruption and similar orientation of the intra-caldera and flank vents suggest that a single E-SE trending dike fed all vents. The intra-caldera lava (which erupted early in the eruption) shows no influence of the 1979 magma; instead, its composition is similar to the last-erupted flank lava. This suggests that the dike split into at least two separate segments, one advanced towards the caldera, where it disaggregated and entrained cumulates from a shallow, subcaldera cumulate crystal mush body. The other branch intruded towards the southeast flank where it intercepted the 1979 reservoir just prior to eruption (Fig. 13). The 1979 end-member decreased from 90% to 0% over the first 19 days of the eruption, indicating that once the two magmas intersected, they mixed progressively until the 1979 reservoir was diluted.

The process of mixing with pre-existing magma at shallow depths has been described for compositional variations observed in Hawaiian eruptions (Wright and Fiske, 1971). For example, over the course of the first two years of the Pu'u O'o eruption, new mafic magma mixed with older differentiated magmas to produce the first 20 episodes of the eruption (e.g. Garcia et al. 1992, 1996). Similarly, during the first days of the 1991–1993 eruption of Etna, new magma intersected and mixed with magma stored in the feeder system (Armienti et al. 1994).

Evidence for mixing provides insight into the internal magma systems in ocean island volcanoes, where eruptions occur fairly frequently (e.g. approximately 45 recorded eruptions in the Galápagos Islands during the last 100 years, Simkin and Siebert 2000). Mixing of shallow-stored magmas with new mafic injections suggests that after initial eruption, the volume of magma is sufficiently large that it can remain molten and not crystallize significantly for years to decades (19 years in the case of the 1979 Cerro Azul magma). This may be a common and important process in ocean island volcanism, especially where eruptions are focused into concentrated rift zones, as is the case in Hawaii, as well as for volcanoes like Cerro Azul that lack rift zones but where consecutive eruptions have occurred from the same sector of the volcano.

Volume constraints of 1979 magma

The transition from early mixing between 1979 and 1998 magmas to late crystal accumulation occurred at least by day 25 of the 5-week eruption. From field evidence and mass balance calculations, it appears that the bulk of the 1979 magma was flushed through the system by the 19th day of the eruption. The rate at which the 1979 magma was mixed can be extrapolated from physical constraints on the volume of lava erupted from the flank vent. There is no chemical evidence for consumption of 1979 material in lava erupted in the caldera, so it is not included in calculations.

The total volume of lava emplaced on the flank of Cerro Azul is estimated to be 1.1×10^8 m^3 (based on field mapping and DEM comparison before and after the eruption; P. Mouginis-Mark, personal communication). Fifteen centimeters of subsidence were observed through November 1998 (Amelung et al. 2000), but the deformation data do not bracket the eruption closely enough to permit estimation of the pre-eruptive magma volume. Mapping suggests that magmas with mixing signatures constitute approximately 90% of the total volume of lava erupted. The average eruption rate for the first 20 days of the eruption is approximately 500,000 m^3/day. If the proportions of the two lava end members erupted from

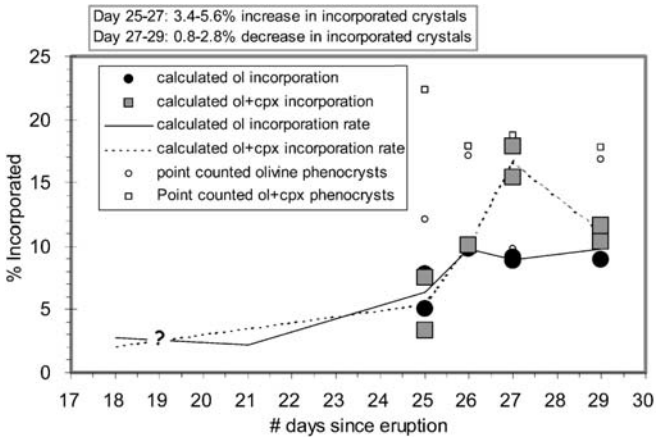

Fig. 14 Crystal incorporation rates for olivine and clinopyroxene by eruption date indicating maximum 5.6% crystal accumulation per day

day 8 (90% 1979 composition) to day 13 (30% 1979 composition) are extrapolated to the 19th day of the eruption, a total of 50×10^6 m^3 of 1979 lava is calculated to have been consumed in the first 13 days of the 1998 eruption. This should be considered a conservative estimate, because eruption rates were visibly higher earlier in the eruption when the proportion of 1979 magma was highest.

Crystal incorporation rates

The rates at which olivine and clinopyroxene were disaggregated from a cumulate mush and incorporated into the 1998 magma of the later erupted lavas was determined by least squares mass balance calculations (Table 5). Proportions of crystals incorporated by the 1998 magma (in terms of the total proportion of olivine plus clinopyroxene) are plotted on Fig. 14 by the date of the eruption of each sample. Prior to day 25, calculated crystal incorporation rates are very low (0.6% per day). The maximum crystal incorporation rate indicates entrained crystals increased by 5.6% per day between day 25 and day 27 of the eruption (Fig. 14). From day 27 through day 29 (the date of emplacement for the last well-constrained sample from the 1998 eruption) incorporation rates decrease by 2.8% per day.

A long-duration eruption at Lanzarote in the Canary Islands from 1730–1736 produced a range of lava compositions, even within individual (month-long) phases of the eruption (Carracedo et al. 1992). Progressive incorporation of peridotite inclusions during the first phase of the Lanzarote eruption is analogous to the incorporation of the olivine and clinopyroxene crystals during the later stages of the 1998 Cerro Azul eruption. These eruptions illustrate that crystal incorporation can occur over days (e.g. Cerro Azul) or years (e.g. Lanzarote). The main difference is that in Cerro Azul, we observed no multigranular xenoliths.

Conclusions

Field observations, whole rock compositions and mineral compositions indicate that the eruption rate and petrogenesis of lavas from the 1998 eruption at Cerro Azul occurred in two stages. Mixing between the 1998 magma and the 1979 magma storage reservoir produced the bulk of the volume of erupted lava. No 1979 component can be traced beyond the 18th day of the eruption. Later erupted lavas were produced by the 1998 magma disaggregating and incorporating olivine and clinopyroxene crystals from a cumulate mush. Intra-caldera lavas show no evidence of the 1979 magma component, indicating the 1979 magma was present only beneath the flank vent, but did not underlie the caldera.

Field observations recorded during the eruption permit estimation of the shallow level mixing and crystal incorporation rates and processes of the 1998 magma to be put in temporal context, because the emplacement chronology of lavas was documented. Multiple petrogenetic processes and incorporation of shallow level magmas may be common at other ocean island volcanoes (e.g. Garcia et al. 1992; Carracedo et al. 1992; Rowland and Munro 1993; Rhodes 1996), but heterogeneous lava flows in the Galápagos Islands have not previously been reported, probably due to limited sampling of individual flows. Also, with the exception of Cerro Azul, and possibly Volcán Ecuador (Geist et al. 2002), most of the western Galápagos shields are characterized by exceedingly limited compositional variation over the entire volcano (Allan and Simkin, 2000; Reynolds and Geist, 1995). Nevertheless, it is important to recognize that single samples may not represent the compositional diversity of an entire lava flows or individual volcanic events. The complex, short time-scale, shallow level processes required to generate the 1998 lavas indicate that detailed study of single flows are needed to characterize the petrogenetic processes of other ocean-island lavas. Surely other eruptive centers experience similar processes, so intra-eruption compositional variations should be considered in combination with larger-scale processes in discussions of the petrogenesis of oceanic magmas.

Acknowledgements This work was funded by NSF grant EAR9612110 to DG; we especially want to thank the Program Directors for providing emergency funding that permitted Teasdale to be on-site within a few days of the start of the eruption. Work was also supported by the NSF under Grant No 9996141. Fieldwork was generously supported by the logistical coordination of the Charles Darwin Research Station and the Galápagos National Park Service. Howard Snell, Heidi Snell, Eduardo Villema, Monica Segovia, and Andres "Gorky" Ruiz were especially helpful in the field. Peter Mouginis-Mark provided images throughout the eruption and preparation of this manuscript. Diane Johnson and Scotty Cornelius of the WSU Geoanalytical lab provided great help with XRF and microprobe analyses. Additional microprobe analyses were completed at the University of Oregon Micro-analytical facility with the help of Michael Shaffer. This paper benefited significantly from reviews by Bill White, Mike Rhodes and Mike Garcia.

References

Allan JA, Simkin T (2000) Fernandina Volcano's evolved, well-mixed basalts; mineralogical and petrological constraints on the nature of the Galapagos plume. J Geophys Res 105:6017–6041

Amelung F, Jónsson S, Zebker H, Segall P (2000) Widespread uplift and 'trapdoor' faulting on Galápagos volcanoes observed with radar interferometry. Nature 407:993–996

Armienti P, Clocchiatti R, D'Orazio M, Innocenti F, Petrini R, Pompilio M, Tonarini S, Villari L (1994) The long-standing 1991–1993 Mount Etna eruption: Petrography and geochemistry of lavas. Acta Volcan 4:15–28

Carracedo JC, Rodriguez-Badiola E, Soler V (1992) The 1730–1736 eruption of Lanzarote, Canary Islands: A long, high-magnitude basaltic fissure eruption. J Volcanol and Geotherm Res, 53:239–250

Chadwick WW, Dietrich JH (1995) Mechanical modeling of circumferential and radial dike intrusion on Galápagos volcanoes. J Volcanol and Geotherm Res 66:37–52

Chadwick WW, Howard KA (1991) The pattern of circumferential and radial eruptive fissures on the volcanoes of Fernandina and Isabela Islands, Galápagos. Bull Volcanol 53:259–275

Clague DA and Denlinger RP (1994) Role of olivine cumulate in destabilizing the flanks of Hawaiian volcanoes. Bull Volcanol 56:425–434

Clague DA, Moore JG, Dixon JE, Friesen WB (1995) [CE1]J Petrol 36:299–349

Ellisor R (1998a) Flank and caldera fissure eruption; helicopter tortoise-rescue. Bulletin of the Global Volcanism Network 23:08

Ellisor R (1998b) Flank and caldera eruptions continue. Bulletin of the Global Volcanism Network 23:09

Ellisor R, Geist D (1999) 1998 eruption at Cerro Azul, Galápagos Islands (abstract, American Geophysical Union, Fall Meeting. EOS Transactions, 80: F1089

Feighner MA, Richards MA (1994) Lithospheric structure and compensation methods of the Galapagos archipelago. J Geophys Res 99:6711–6729

Garcia MO, Rhodes JM, Ho R, Ulrich G, Wolfe E (1992) Petrology of lavas from episodes 2–47 of the Pu'u O'o eruption of Kilauea Volcano, Hawaii: Evaluation of magmatic processes. Bull Volcanol 55:1-16.

Garcia MO, Hulsebosch TP, Rhodes JM (1995) Olivine-rich submarine basalts from the southwest rift zone of Mauna Loa volcano: Implications for magmatic processes and geochemical evolution. In: Rhodes JM, Lockwood JP (eds) Mauna Loa revealed, structure, composition, history and hazards. Geophysical Monograph 92, American Geophysical Union, Washington DC, pp 219–239

Garcia MO, Rhodes JM, Trusdell FA, Pietruszka AJ (1996) Petrology of Lavas from the Pu'u O'o eruption of Kilauea Volcano: III. The Kupaianaha episode (1986–1992). Bull Volcanol 58:359–379

Garcia MO (1996) Petrography and olivine and glass chemistry of lavas from the Hawaii Scientific Drilling Project. J Geophys Res 101:11701–11713

Geist D, Howard KA, Jellinek AM, Rayder S (1995a) The volcanic history of Volcán Alcedo, Galápagos Archipelago: A case study of rhyolitic oceanic volcanism. Bull Volcanol 56:243–260

Geist D, Howard KA, Larson P (1995b) The generation of oceanic rhyolites by crystal fractionation: The basalt-rhyolite association at Volcán Alcedo, Galápagos Archipelago J Petrol 36:965–982

Geist D, Naumann T, Larson P (1998) Evolution of Galápagos magmas: mantle and crustal fractionation without assimilation. J Petrol 39:953–971

Geist D, White WM, Albarede F, Harpp K, Reynolds R, Blichert-Toft J, Kurz M (2002) Volcanic evolution in the Galápagos: The dissected shield of Volcan Ecuador. Geochemistry Geophysics Geosystems, 3:1-32

Ghiorso MS, Sack RO (1995) Chemical mass transfer in magmatic systems IV. A revised and internally consistent thermodynamic model for the interpolation and extrapolation of liquid-solid equilibria in magmatic systems at elevated temperatures and pressures. Contrib Mineral Petrol 119:197–212

Helz RT (1987) Differentiation behavior of Kilauea Iki lava lake, Kilauea Volcano, Hawaii: An overview of past and current work. In: Mysen BO (ed) Magmatic processes: physicochemical principles. The Geochemical Society, Spec Publ No. 1, pp 241–258

Hoffman AW, Feigenson MD, Raczek I (1984) Case studies on the origin of basalt III. Petrogenesis of the Mauna Ulu eruption, Kilauea, 1969–1971. Contrib Mineral Petrol 88:24–35

Johnson DM, Hooper PR, Conrey RM (1999) XRF analysis of rocks and minerals or major and trace elements on a single low dilution Li-tetraborate fused bead. Advances in X-ray Analysis 41: 843–867

Kurz M, Geist D (1999) Dynamics of the Galápagos hotspot from Helium isotope geochemistry. Geochim Cosmochim Acta 63:4139–4156

Lipman P Mullineaux, DR (1981) The 1980 eruptions of Mount St. Helens. USGS Professional Paper 1250

Mouginis-Mark PJ, Snell H, Ellisor R (2000) GOES satellite and field observations of the 1998 eruption of Volcán Cerro Azul, Galápagos Islands. Bull Volcanol 62:188–198

Naumann T, Geist D (2000) Physical volcanology and structural development of Cerro Azul Volcano, Isabela Island, Galápagos: implications for the development of Galápagos -type shield volcanoes. Bull Volcanol 61:497–514

Naumann T, Geist D, Kurz M (2002) Petrology and geochemistry of Cerro Azul Volcano and the origin of the petrologic diversity of the Western Galápagos shield volcanoes. J Petrol 43:859–883

Naumann T (1998) Geology and petrology of Cerro Azul Volcano, Isabela Island, Galápagos Archipelago. PhD Dissertation, University of Idaho, Moscow, 153pp

Newhall CG Punongbayan RS (1996) Fire and Mud: Eruptions and Lahars of Mount Pinatubo, Philippines. University of Washington Press, Seattle

Putirka K, Johnson M, Kinzler R, Longhi J, Walker D (1996) Thermobarometry of mafic igneous rocks based on clinopyroxene-liquid equilibria, 0–30 kbar. Contrib Mineral Petrol 123:92–108

Reiners PW (2002) Temporal-compositional trends in intraplate basaltic eruptions: Implications for mantle heterogeneity and melting zone structure. Geochemistry Geophysics Geosystems 3:1-30

Reynolds RW, Geist DJ (1995) Petrology of lavas from Sierra Negra volcano, Isabela Island, Galápagos archipelago. J Geophys Res 100:24537–24553

Roeder PL, Emslie RF (1970) Olivine-liquid equilibrium. Contrib Mineral Petrol 29:275–289

Rhodes JM (1996) Geochemical stratigraphy of lava flows sampled by the Hawaii Scientific Drilling Project. J Geophys Res 101:11729–11746

Rowland SK, Munro DC (1993) The 1919–1920 eruption of Mauna Iki, Kilauea: Chronology, geologic mapping, and magma transport mechanisms. Bull Volcanol 55:190–203

Simkin T, Siebert L (2000) Appendix 2: Catalog of historically active volcanoes on earth. In: Sigurdsson H (ed) Encyclopedia of Volcanoes. Academic Press, San Diego, pp 1365–1383

Sparks RJ, Sigurdsson H, Wilson L (1977) Magma mixing: A mechanism for triggering acid explosive eruptions. Nature 267:315–318

Standish J, Geist D, Harpp K, Kurz MD (1998) The emergence of a Galápagos shield Volcano, Roca Redonda. Contrib Mineral Petrol 133:136–148

Ulmer P (1989) The dependence of the Fe^{2+} - Mg cation-partitioning between olivine and basaltic liquid on pressure, temperature and composition. Contrib Mineral Petrol 101:261–273

White WM, McBirney AR, Duncan RA (1993) Petrology and geochemistry of the Galápagos Islands: Portrait of a pathological mantle plume. J Geophys Res 98:19533–19563

Wright TL, Fiske RS (1971) Origin of the differentiated and hybrid lavas of Kilauea volcano, Hawaii. J Petrol 12:1-65